Effects of NH3 and alkaline metals on the formation of particulate sulfate and nitrate in wintertime Beijing

Huang, Ru-Jin; Duan, Jing; Li, Yongjie; Chen, Qi; Chen, Yang; Tang, Mingjin; Yang, Lu; Ni, Haiyan; Lin, Chunshui; Xu, Wei

Published in:
Science of the Total Environment

DOI:
10.1016/j.scitotenv.2020.137190

Publication date:
2020

Science of the Total Environment 717 (2020) 137190

Contents lists available at ScienceDirect

Science of the Total Environment

journal homepage: www.elsevier.com/locate/scitotenv

Effects of NH_3 and alkaline metals on the formation of particulate sulfate and nitrate in wintertime Beijing

Ru-Jin Huang [a,*], Jing Duan [a], Yongjie Li [b,*], Qi Chen [c,*], Yang Chen [d], Mingjin Tang [e], Lu Yang [a], Haiyan Ni [a,f], Chunshui Lin [a,g], Wei Xu [a,g], Ying Liu [h], Chunying Chen [h], Zhen Yan [i], Jurgita Ovadnevaite [g], Darius Ceburnis [g], Uli Dusek [f], Junji Cao [a], Thorsten Hoffmann [j], Colin D. O'Dowd [g]

[a] Key Laboratory of Aerosol Chemistry and Physics, State Key Laboratory of Loess and Quaternary Geology, CAS Center for Excellence in Quaternary Science and Global Change, Institute of Earth and Environment, Chinese Academy of Sciences, Xi'an 710061, China
[b] Department of Civil and Environmental Engineering, Faculty of Science and Technology, University of Macau, Taipa, Macau, China
[c] State Key Joint Laboratory of Environmental Simulation and Pollution Control, College of Environmental Sciences and Engineering, Peking University, Beijing, China
[d] Chongqing Institute of Green and Intelligent Technology, Chinese Academy of Sciences, Chongqing 400714, China
[e] State Key Laboratory of Organic Geochemistry and Guangdong Key Laboratory of Environmental Protection and Resources Utilization, Guangzhou Institute of Geochemistry, Chinese Academy of Sciences, Guangzhou, China
[f] Centre for Isotope Research (CIO), Energy and Sustainability Research Institute Groningen (ESRIG), University of Groningen, the Netherlands
[g] School of Physics and Centre for Climate and Air Pollution Studies, Ryan Institute, National University of Ireland Galway, University Road, Galway, Ireland
[h] CAS Key Laboratory for Biological Effects of Nanomaterials and Nanosafety, National Centre for Nanoscience and Technology, Beijing 100191, China
[i] Metrohm China Ltd., Shanghai 200335, China
[j] Institute of Inorganic and Analytical Chemistry, Johannes Gutenberg University of Mainz, Duesbergweg 10-14, Mainz 55128, Germany

HIGHLIGHTS

- Alkaline metal ions compete with NH_3 in the neutralization of sulfate and nitrate.
- Increased sulfate was related to low pH, while high pH promotes nitrate formation.
- In some regions the sulfate/nitrate formation might be largely affected by dust.

GRAPHICAL ABSTRACT

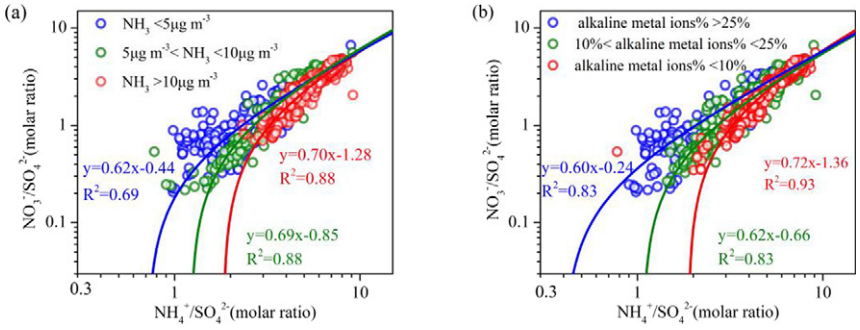

ARTICLE INFO

Article history:
Received 14 December 2019
Received in revised form 5 February 2020
Accepted 7 February 2020
Available online 8 February 2020

Editor: Pingqing Fu

Keywords:
Sulfate

ABSTRACT

Sulfate and nitrate from secondary reactions remain as the most abundant inorganic species in atmospheric particle matter (PM). Their formation is initiated by oxidation (either in gas phase or particle phase), followed by neutralization reaction primarily by NH_3, or by other alkaline species such as alkaline metal ions if available. The different roles of NH_3 and metal ions in neutralizing H_2SO_4 or HNO_3, however, are seldom investigated. Here we conducted semi-continuous measurements of SO_4^{2-}, NO_3^-, NH_4^+, and their gaseous precursors, as well as alkaline metal ions (Na^+, K^+, Ca^{2+}, and Mg^{2+}) in wintertime Beijing. Analysis of aerosol acidity (estimated from a thermodynamic model) indicated that preferable sulfate formation was related to low pH conditions, while high pH conditions promote nitrate formation. Data in different mass fraction ranges of alkaline metal ions showed that in some ranges the role of NH_3 was replaced by alkaline metal ions in the neutralization reaction

* Corresponding authors.
E-mail addresses: rujin.huang@ieecas.cn (R.-J. Huang), yongjieli@um.edu.mo (Y. Li), qichenpku@pku.edu.cn (Q. Chen).

https://doi.org/10.1016/j.scitotenv.2020.137190

Nitrate
Ammonia
Alkaline metals

of H_2SO_4 and HNO_3 to form particulate SO_4^{2-} and NO_3^-. The relationships between mass fractions of SO_4^{2-} and NO_3^- in those ranges of different alkaline metal ion content also suggested that alkaline metal ions participate in the competing neutralization reaction of sulfate and nitrate. The implication of the current study is that in some regions the chemistry to incorporate sulfur and nitrogen into particle phase might be largely affected by desert/fugitive dust and sea salt, besides NH_3. This implication is particularly relevant in coastal China and those areas with strong influence of dust storm in the North China Plain (NCP), both of which host a number of megacities with deteriorating air quality.

1. Introduction

Secondary formation contributes substantially to atmospheric particulate matter (PM) in urban China (Huang et al., 2014a). Formation of the abundant secondary inorganic aerosol (SIA), including sulfate, nitrate, and ammonium (or collectively SNA), is more complex than mere one-step oxidation or neutralization reaction of their respective gaseous precursors SO_2, NO_x (= NO + NO_2), and NH_3. As for sulfate formation from SO_2, some studies suggested that at least in summer gas-phase oxidation by OH radicals can explain the sulfate production (Takegawa et al., 2009; Xiao et al., 2009), and others also reported that aqueous-phase oxidation is more important in some conditions (Sun et al., 2013, 2014; Yang et al., 2015; B. Zheng et al., 2015; G.J. Zheng et al., 2015). Regardless of the formation route, the so-formed sulfuric acid (H_2SO_4) or sulfate are extremely non-volatile and will participate in nucleation (for H_2SO_4) and mostly stay in the particle phase (mostly as $(NH_4)_2SO_4$ or NH_4HSO_4) (Seinfeld and Pandis, 2016). The form of existence of these sulfur species (sulfate, bisulfate, or sulfuric acid) has implications on aerosol mass, hygroscopicity and acidity (Martin, 2000; Silvern et al., 2017), given their high abundance. As for nitrate formation from NO_x, gas-phase oxidation by OH radicals (Hertel et al., 2012; Ge et al., 2017) and heterogeneous reactions of N_2O_5 (Dall'Osto et al., 2009; Pathak et al., 2009; Tang et al., 2012) are believed to be important pathways during day and night, respectively. The so-formed nitric acid (HNO_3) and ammonium nitrate (NH_4NO_3) are both subject to gas-particle partitioning (Ansari and Pandis, 2000; Seinfeld and Pandis, 2016) because of their high volatility (for HNO_3) and thermal lability (for NH_4NO_3). Recognizing the importance of aqueous-phase and heterogeneous processes in formation of particulate sulfate and nitrate, model prediction of these species in China has been dramatically improved (B. Zheng et al., 2015; G.J. Zheng et al., 2015, J. Zheng et al., 2015; Chen et al., 2016).

As the most abundant alkaline gas in the atmosphere, NH_3 is principally responsible for neutralization reaction of H_2SO_4 and HNO_3 to form particulate nitrate and sulfate (Sharma et al., 2007; Hu et al., 2008; Behera and Sharma, 2010; Ye et al., 2011; Behera et al., 2013). These neutralization reactions are also the main driving force to shift NH_3 to the particle phase, thus mediating the NH_3 distribution between the gas and particle phases. There are, however, other alkaline species in the atmosphere that might compete with NH_3 for acidic gases. For example, calcium (Ca^{2+}) and magnesium (Mg^{2+}) in desert or fugitive dust (Zhang et al., 2014), potassium (K^+) in biomass burning aerosol (Ryu et al., 2007), and sodium (Na^+) in sea salt, if present, may also combine with H_2SO_4 and HNO_3 and form corresponding salts (Yao et al., 2001; L. Wang et al., 2013; Allen et al., 2015). Further, reduced organic nitrogen species such as amines (Ge et al., 2011; Huang et al., 2012; Zhang et al., 2012; Huang et al., 2014b; J. Zheng et al., 2015) might alternatively be the neutralizing agent for those acidic gases. However, there is little investigation on the competition between the most studied NH_3 and other alkaline species in particulate sulfate and nitrate formation (Guo et al., 2018; Vasilakos et al., 2018; Nenes et al., 2019). Given the large number of megacities in eastern coastal China where sea salt influence can be significant and the severely polluted megacities in northwest China where dust influence is strong, such investigation is highly desirable.

In the atmosphere, all these chemical processes mentioned above are most likely intertwined and may affect each other. To better understand factors affecting SNA formation, simultaneous measurements of SNA and their precursors, as well as other alkaline species that may affect their formation are needed. In addition, those intertwined processes occur rapidly in the dynamic atmospheric system, imposing another challenge for interpretation of time-integrated data, for instance, those obtained from daily samples. Traditionally, SNA species and/or their precursors were measured with off-line approaches, yielding data with time resolutions of a day or more. The applications of real-time methods based on semi-continuous ion chromatography or direct mass spectrometry (Li et al., 2017b) provide unprecedented advantages with high time resolutions and large datasets. These applications result in rich information for the investigation of the chemical transformation and thermodynamic behaviors in SNA formation (Takegawa et al., 2009; Xiao et al., 2009; Du et al., 2010; Kong et al., 2014; Sun et al., 2013, 2014; Griffith et al., 2015; Tan et al., 2017). Despite recent advances that elaborate the time-resolved transformation of SNA via diurnal or seasonal analyses, relatively little attention is paid to the competition between sulfate and nitrate formation and the influence by alkaline species such as alkaline metal ions (also defined as nonvolatile cations (NVCs) in some studies) (L. Wang et al., 2013; Kong et al., 2014; Guo et al., 2018; Pye et al., 2019).

In this study, we present results of simultaneous measurements of SNA and their precursors as well as major alkaline species including Na^+, K^+, Ca^{2+}, and Mg^{2+} in wintertime Beijing. The objective is to elucidate the relationships between particulate sulfate/nitrate and ammonia/ammonium abundance, content of other alkaline ions, as well as thermodynamic properties such as aerosol acidity. Implications from the findings are also discussed regarding the increasing interest on NH_3 emissions in China.

2. Materials and methods

2.1. Observation site

Measurements were carried out on the roof of a ~20 m height building of the National Center for Nanoscience (39.99°N, 116.32°E) in Beijing, China. The measurement site in Haidian district is close to the fourth ring road of Beijing, and is surrounded by residential, commercial and traffic areas. Measurements were performed from 23 January to 28 February 2015.

2.2. Measurements

An NH_3 analyzer (G2103, Picarro, USA) was employed to measure ambient concentration of NH_3. This analyzer uses wavelength-scanning optical cavity ring down spectroscopy (WS-CRDS) which is capable of measuring NH_3 with a parts-per-trillion (ppt) sensitivity based on a sophisticated time-based measurement system (Maasikmets et al., 2015). The G2103 is equipped with high-precision temperature and pressure control systems to ensure the highest accuracy and lowest drift. In addition, the G2103 offers a large dynamic range, providing linear response into the parts-per-million (ppm) range without dilution, concentration and sample preparation.

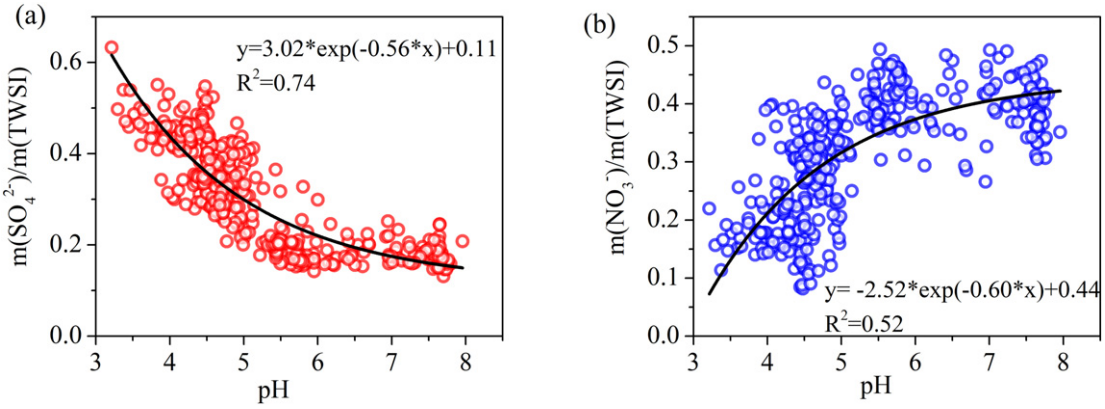

Fig. 1. Correlations between predicted aerosol pH and the mass fractions of sulfate (a) and nitrate (b), Note that m (TWSI) is the mass concentration of total water-soluble ions including Na^+, K^+, Mg^{2+}, Ca^{2+}, NH_4^+, SO_4^{2-}, NO_3^-, Cl^-.

In parallel with the NH_3 analyzer, another real-time instrument, a monitor for aerosols and gases in ambient air (MARGA ADI 2080, Metrohm Applikon, Switzerland) was deployed. The MARGA system with a $PM_{2.5}$ cyclone inlet was applied to measure the mass concentrations of main water-soluble inorganic species (including NH_4^+, SO_4^{2-}, NO_3^-, Cl^-, Na^+, K^+, Ca^{2+} and Mg^{2+}) and related trace gaseous species (HCl, HNO_2, SO_2, HNO_3 and NH_3) simultaneously. MARGA has been widely used to measure particulate inorganic species and trace gases at a one-hour time resolution (Rumsey et al., 2014; Nie et al., 2015). Details about MARGA were described elsewhere (ten Brink et al., 2007; Du et al., 2010; Du et al., 2011). Briefly, the MARGA system is composed of a sampling unit and an analysis unit. In the sampling unit, gaseous species are absorbed and dissolved in 0.0035% H_2O_2 solution on a wet rotary denuder (WRD), while particulate species are collected by a steam jet aerosol collector (SJAC). Both gaseous and particulate species collected as liquid (aqueous) samples are subsequently analyzed by ion chromatography. An internal calibration standard was continuously injected over the entire observation period to account for any changes in the system. External standard solutions were also used to ensure successful peak identification and data quality. Comparison experiments between MARGA and filter-based methods suggested that sampling efficiency of MARGA is sufficient for ambient monitoring (Khlystov et al., 1995; Chow and Watson, 1998). The detection limits are <0.015 ppb for aerosol anions (or 0.064 μg m^{-3} for SO_4^{2-}, 0.042 μg m^{-3} for NO_3^-, 0.022 μg m^{-3} for Cl^-) and acidic trace gases (or 0.024 μg m^{-3} for HCl, 0.031 μg m^{-3} for HNO_2, 0.043 μg m^{-3} for SO_2, 0.042 μg m^{-3} for HNO_3), and < 0.118 ppb for NH_4^+ (or 0.095 μg m^{-3}) and NH_3(or 0.090 μg m^{-3}) (Trebs et al., 2004). Here we used the NH_3 data from Picarro and aerosol ions data from MARGA for our analysis. In addition, a Thermo Scientific Model 42i NO-NO_2-NO_x analyzer was used to measure NO and NO_2 concentrations.

Hourly meteorological dataset including relative humidity (RH) and temperature were measured with an automatic weather station (MAWS301, Vaisala, Finland). Maintenance of either the Picarro NH_3 analyzer or MARGA led to some loss of data (capture rate of 71.4%). Herein, we only considered data points where concentrations of major species were all available (624 hourly data points).

2.3. Thermodynamic model

The thermodynamic model ISORROPIA-II was used to estimate the thermodynamic equilibrium state of the NH_4^+-SO_4^{2-}-NO_3^--Cl^--Na^+-K^+-Ca^{2+}-Mg^{2+} system (Fountoukis and Nenes, 2007; Song et al., 2018). The model outputs, including hydronium ion concentration (H^+_{air}) and liquid water content (W), were used to calculate the in situ pH according to Guo et al. (2015):

$$\mathrm{pH} = -\log_{10}\gamma_{H^+}H^+_{aq} = -\log_{10}\frac{1000\gamma_{H^+}H^+_{air}}{W_i + W_o} \cong -\log_{10}\frac{1000\gamma_{H^+}H^+_{air}}{W_i} \quad (1)$$

where γ_H^+ is the activity coefficient of hydronium ion (assumed to be unity), H^+_{aq} (mol L^{-1}) is the concentration of hydronium ion in particle

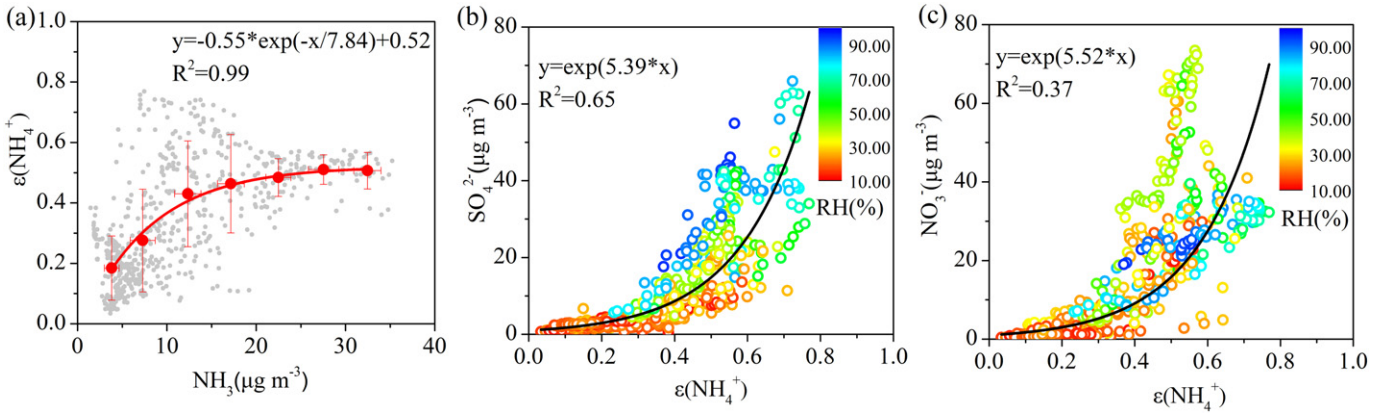

Fig. 2. Relationship between $\varepsilon(NH_4^+)$ and mass concentration of gaseous NH_3 (a), between mass concentration of sulfate and $\varepsilon(NH_4^+)$ colored by RH (b), and between mass concentration of nitrate and $\varepsilon(NH_4^+)$ colored by RH (c). See main text for the definition of $\varepsilon(NH_4^+)$.

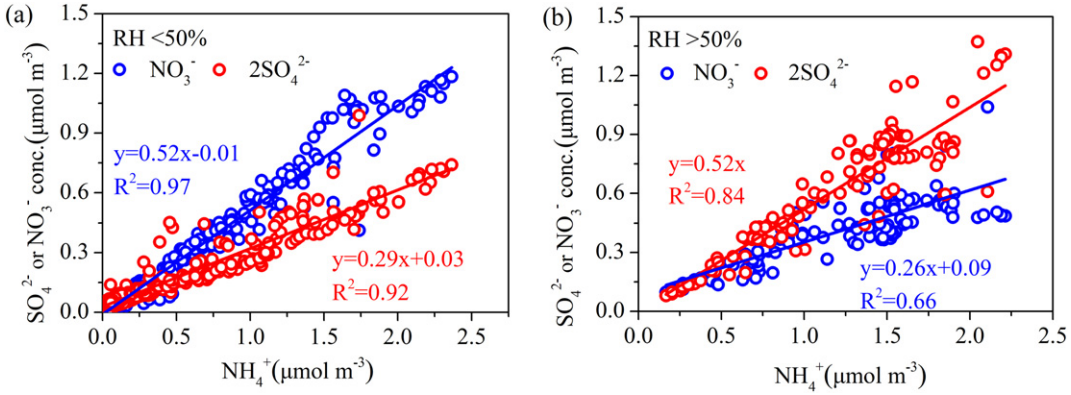

Fig. 3. Correlations between equivalent concentrations of sulfate and nitrate and that of ammonium in ambient RH <50% (a) and >50% (b).

liquid water, H^+_{air} (μg m^{-3}) is the mass concentration of hydronium ion in air, and W_i and W_o (μg m^{-3}) is the water concentration of bulk particle related to inorganic and organic species, respectively. Since Battaglia et al. (2019) have showed that organics do not likely influence aerosol pH significantly in Beijing, we only consider the portion of liquid water contributed by inorganic species (W_i).

Previous studies have revealed that pH prediction by thermodynamic models can lead to large model bias in the "reverse" mode, where only particulate species are used as model inputs (Guo et al., 2015; Hennigan et al., 2015). On the other hand, H^+ is unstable in an efflorescent particle condition (Hennigan et al., 2015). Therefore, we ran ISORROPIA-II in "forward" mode, where both gaseous and particulate species were used as model inputs. We also ran ISORROPIA-II in "metastable" mode, where particles were assumed to be deliquescent and there is no solid formation (Fountoukis and Nenes, 2007). The accuracy of model simulation and pH prediction is evaluated by comparing the modeled and measured partitioning of NH_3(gas)-NH_4^+(particle) which are highly sensitive to pH, temperature and RH (Guo et al., 2016). As shown in Fig. S1, the measured and modeled values correlate well, suggesting that the accuracy of the ISORROPIA-II model is acceptable.

3. Results and discussion

3.1. Aerosol acidity and sulfate, nitrate formation

As shown in Fig. 1, the relationship between aerosol pH and the mass fraction of SO_4^{2-} is opposite to the relationship between aerosol pH and the mass fraction of NO_3^-. A positive correlation between pH and the mass fraction of nitrate whereas a negative correlation between pH and the mass fraction of sulfate were observed. This observation implies that nitrate formation is preferred when aerosol acidity is low (high pH), while sulfate will probably dominate the secondary inorganic aerosol when aerosol acidity is high (low pH). Sulfate is the primary driver of aerosol pH/acidity and therefore, with less sulfate the aerosol pH may increase, a condition that is inducive for NO_3^- formation by reactions between HNO_3 and NH_3. This result may also be helpful in understanding the partitioning of semi-volatile species (HNO_3/NO_3^-) between the gas and particle phases, which are affected by various factors such as temperature, RH and aerosol acidity (Guo et al., 2015). Low aerosol pH will drive NO_3^- to form HNO_3 (a protonated and volatile state), thus the partitioning of HNO_3/NO_3^- is shifted from the particle phase to the gas phase, preventing the formation of NH_4NO_3 in the particle phase (Mentel et al., 1999; Griffith et al., 2015). This shifting will lead to a lower level of particulate NO_3^- and a higher mass fraction of sulfate based on their competition for ammonium. In contrast, when pH increases, the low aerosol acidity will keep NO_3^- into the particle phase, leading to a higher mass fraction of nitrate in the particle phase.

3.2. Competition for ammonia in the formation of sulfate and nitrate

Fig. 2a shows the partitioning ratio of ammonium ($\varepsilon(NH_4^+)$) as a function of NH_3 concentration. $\varepsilon(NH_4^+)$ can be calculated as follows:

$$\varepsilon(NH_4^+) = \frac{[NH_4^+]}{([NH_4^+] + [NH_3])} \quad (2)$$

where $[NH_4^+]$ is the molar concentration of particulate ammonium (μmol m^{-3}) and $[NH_3]$ is the molar concentration of gaseous ammonia (μmol m^{-3}). The gas-aerosol partitioning of ammonia appears to be dependent on the concentration of NH_3 until concentrations higher than 25 μg m^{-3} are reached and the partitioning ratio is constant at around 0.5. The amounts of NH_3 partitioned into the particle phase are largely affected by the availability of H_2SO_4 and HNO_3. In turn, concentrations of particulate sulfate and nitrate are also affected by the partitioning ratio of NH_3. Fig. 2b and c show similar exponential increases of sulfate and nitrate as a function of $\varepsilon(NH_4^+)$, respectively, suggesting high availability of NH_3 might facilitate the incorporation of sulfate and nitrate into the particle phase, especially for nitrate that is semi-volatile. As shown in Fig. 2b, at the same $\varepsilon(NH_4^+)$ level, more sulfate is formed under higher RH conditions, consistent with previous studies that demonstrated the exponential production of sulfate with increasing RH (e.g., Sun et al., 2013, 2014; Wang et al., 2016). In contrast to sulfate, nitrate did not show a clear increasing correlation with RH in the whole RH range (Fig. 2c), most likely due to influences from both RH and temperature. The thermodynamic equilibrium between NH_3(g) + HNO_3 (g) and particulate NH_4NO_3 is strongly affected by temperature (Seinfeld and Pandis, 2016).

To further investigate the effect of RH on the formation of particulate sulfate and nitrate, we divided data into low- and high-RH (i.e., RH <50% and RH >50%) categories, and showed the relationships between equivalent concentrations of SO_4^{2-} and NO_3^- and that of NH_4^+ (Fig. 3). In the low-RH range (<50%, Fig. 3a), nitrate was the dominant anion to associate with ammonium, while the reverse is true for the high-RH range (>50%, Fig. 3b). It can thus be interpreted that at a given NH_4^+ concentration, more sulfate was formed at high-RH conditions, while more nitrate was formed at low-RH conditions. This observation may hint on distinction in the formation pathways between these two most important particulate anions.

Table 1
SOR, NOR, equivalent concentrations of sulfate and nitrate, and ratio of $NO_3^-/2SO_4^{2-}$ at RH <50% and RH >50%.

RH	SOR	NOR	$2SO_4^{2-}$ (μmol m^{-3})	NO_3^- (μmol m^{-3})	$NO_3^-/2SO_4^{2-}$
<50%	0.14	0.16	0.14	0.19	1.36
>50%	0.55	0.38	0.62	0.41	0.66

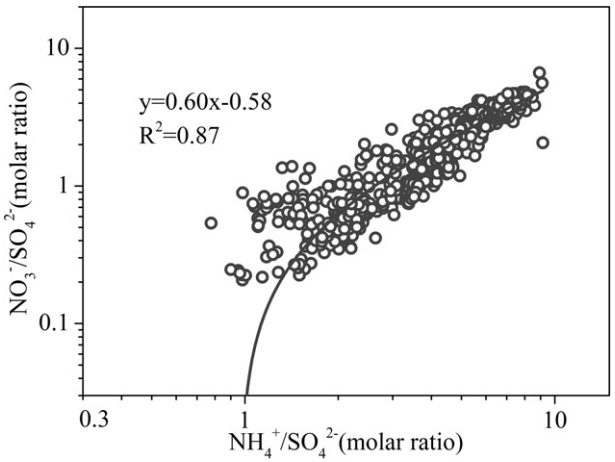

Fig. 4. Correlation between nitrate to sulfate molar ratio and ammonium to sulfate molar ratio.

We use sulfur conversion ratio (SOR) and nitrogen conversion ratio (NOR), respectively, to indicate the degrees of conversion (to particulate species) for sulfur and nitrogen (Khoder, 2002; Tian et al., 2016). SOR and NOR are defined as:

$$SOR = \frac{[SO_4^{2-}]}{[SO_4^{2-}] + [SO_2]} \quad (3)$$

$$NOR = \frac{[NO_3^-]}{[NO_3^-] + [NO_2]} \quad (4)$$

where $[SO_4^{2-}]$ and $[NO_3^-]$ are the molar concentrations of sulfate and nitrate (μmol m^{-3}), respectively, while $[SO_2]$ and $[NO_2]$ are the molar concentrations of sulfur dioxide and nitrogen dioxide (μmol m^{-3}), respectively. The mean values of SOR and NOR are 0.14 and 0.16, respectively, when RH was <50% (Table 1). In addition, a high average ratio of equivalent concentrations of nitrate to sulfate ($NO_3^-/2SO_4^{2-}$ >1) was observed at RH <50% (Table 1), suggesting that NH_4^+ combined more with NO_3^- than with SO_4^{2-}. The same observation is reflected by the slopes between equivalent concentrations of sulfate (0.29) and nitrate (0.52) versus ammonium (Fig. 3a). For high-RH conditions, oxidation of SO_2 can be enhanced, especially through heterogeneous pathways (Sander and Seinfeld, 1976). Similarly, RH can affect NH_3NO_3 partitioning between the gas and particle phases (Willison et al., 1985; Wakamatsu et al., 1996), with more efficient HNO_3 and NH_3 conversion into the particle phase at high RH level where particles deliquesce to form aqueous droplets (Trebs et al., 2004; Trebs et al., 2005). We also observed much higher average SOR and NOR values of 0.55 and 0.38, respectively, when RH was >50% (Table 1). However, from low (<50%) to high RH (>50%), the increase of SOR (4 times) is more prominent than that of NOR (2.4 times), leading to a low average ratio of equivalent concentrations of nitrate to sulfate ($NO_3^-/2SO_4^{2-}$ <1) at high RH, as shown in Table 1. Thus, at high RH (>50%), NH_4^+ combined more with SO_4^{2-} than with NO_3^-. The opposite trend in slopes between equivalent concentrations of sulfate (0.52) and nitrate (0.26) versus ammonium (Fig. 3b) also suggests more efficient formation of sulfate relative to nitrate at high-RH conditions, as discussed in Wang et al. (2016).

3.3. The role of alkaline metals in the formation of sulfate and nitrate

Previous studies have documented that the formation of NH_4NO_3 through homogeneous reaction of NH_3 with HNO_3 is favorable under high-NH_3 and low-sulfate conditions (Pathak et al., 2009; Ianniello et al., 2010). The relationship between the molar ratio of $[NO_3^-]/[SO_4^{2-}]$ and that of $[NH_4^+]/[SO_4^{2-}]$ has been widely used to interpret the formation pathway of particulate nitrate, as sulfate competes with nitrate for ammonium during the formation processes (Huang et al., 2011; Ye et al., 2011; Squizzato et al., 2013). The linear correlation between $[NO_3^-]/[SO_4^{2-}]$ and $[NH_4^+]/[SO_4^{2-}]$ in NH_3-rich conditions indicates the homogenous formation of nitrate (Pathak et al., 2009; He et al., 2012). Field measurements from many sites worldwide have proposed $[NH_4^+]/[SO_4^{2-}]$ ≥1.5 (fully HSO_4^-) or $[NH_4^+]/[SO_4^{2-}]$ ≥2 (fully neutralized SO_4^{2-}) as a NH_3-rich condition for homogeneous formation of NO_3^- (Griffith et al., 2015; Tao et al., 2016). On the other hand, in NH_3-poor conditions, there exist heterogeneous reactions for NO_3^- formation, for example, the hydrolysis of N_2O_5 on preexisting particles (Pathak et al., 2009). Fig. 4 shows that $[NO_3^-]/[SO_4^{2-}]$ was correlated well with $[NH_4^+]/[SO_4^{2-}]$ with a correlation coefficient (R^2) of 0.87, indicating that homogeneous reaction of NH_3 with HNO_3 is an important pathway of NO_3^- formation in our study. However, intercept of the linear regression with the axis of $[NH_4^+]/[SO_4^{2-}] = 0.9$ is much smaller than the NH_3-rich threshold ($[NH_4^+]/[SO_4^{2-}]$ ≥1.5) reported in previous studies (Pathak et al., 2009; He et al., 2012; Squizzato et al., 2013), indicating the existence of some NH_3-poor conditions (i.e., $[NH_4^+]/[SO_4^{2-}]$ <1.5). Consistently, in our study the average concentration of NH_3 at $[NH_4^+]/[SO_4^{2-}]$ <1.5 was 4.1 μg m^{-3}, which was much lower than that at $[NH_4^+]/[SO_4^{2-}]$ >1.5 (12.0 μg m^{-3}).

The influence of NH_3 on the correlation between $[NO_3^-]/[SO_4^{2-}]$ and $[NH_4^+]/[SO_4^{2-}]$ and the pathways of nitrate formation are further investigated. Fig. 5 depicts molar ratio of $[NO_3^-]/[SO_4^{2-}]$ against that of $[NH_4^+]/[SO_4^{2-}]$, segregated by mass concentration of NH_3 (Fig. 5a) and mass fraction of alkaline metal ions (Fig. 5b). Note that the regression line at the highest NH_3 range corresponds to that at the lowest alkaline metal ion range, and vice versa. As also summarized in Table 2, the molar ratio of $[NO_3^-]/[SO_4^{2-}]$ and that of $[NH_4^+]/[SO_4^{2-}]$ are better

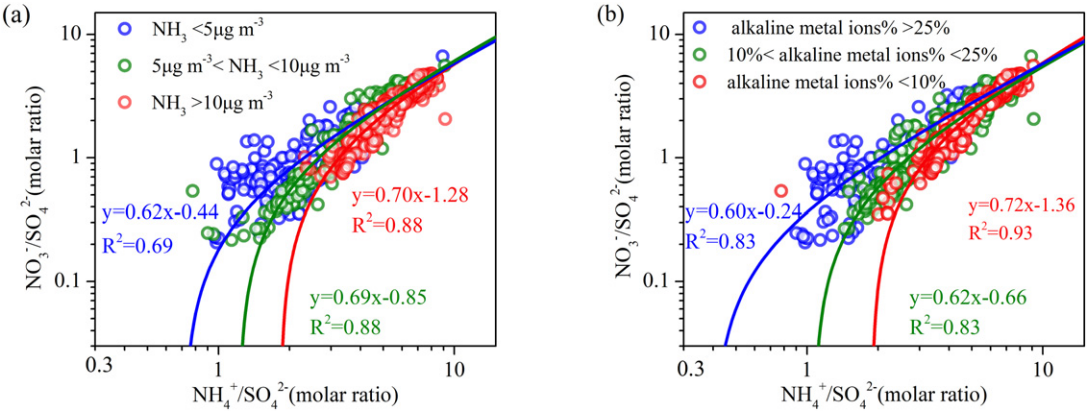

Fig. 5. Correlation between nitrate to sulfate molar ratio and ammonium to sulfate molar ratio as a function of mass concentration of NH_3 (a) and of mass fraction of alkaline metal ions (b).

Table 2
Comparison of the slopes, intercepts and R^2 of the regression lines in Fig. 5, as well as alkaline metal ion content (mass percentage) and mean mass concentration of gases and aerosol species.

	NH_3 (μg m^{-3})			Alkaline ions %		
	<5	5–10	>10	<10	10–25	>25
Slope	0.62	0.69	0.70	0.72	0.62	0.60
Intercept[a]	0.71	1.23	1.83	1.89	1.32	0.40
R^2	0.69	0.88	0.88	0.93	0.83	0.83
Alkaline ions (%)[b]	27.9	18.2	8.6	6.0	15.8	39.2
NH_3 (μg m^{-3})	3.83	7.30	18.65	17.68	7.01	6.11
SO_2 (μg m^{-3})	10.69	18.40	43.80	42.68	19.68	10.39
NO_2 (μg m^{-3})	13.04	24.32	42.36	39.46	21.12	22.53
NH_4^+ (μg m^{-3})	0.94	4.07	18.73	19.72	2.88	1.06
SO_4^{2-} (μg m^{-3})	2.31	5.35	20.54	22.03	3.92	1.89
NO_3^- (μg m^{-3})	1.11	6.32	27.51	28.97	4.15	1.82
Cl^- (μg m^{-3})	0.36	1.54	6.85	6.68	1.53	0.76
Na^+ (μg m^{-3})	0.08	0.16	0.43	0.42	0.15	0.12
K^+ (μg m^{-3})	0.15	0.45	2.31	2.24	0.49	0.25
Mg^{2+} (μg m^{-3})	0.25	0.51	0.59	0.53	0.42	0.45
Ca^{2+} (μg m^{-3})	1.08	1.39	1.88	1.49	1.07	2.40
TWSI (μg m^{-3})	6.29	19.80	78.84	82.09	14.61	8.73
RH (%)	22	26	50	51	25	22
T (K)	273.3	275.5	276.0	276.4	275.2	276.2

[a] Intercept value of $[NH_4^+]/[SO_4^{2-}]$.
[b] Mass percentage of alkaline metal ions (%) = $(Na^+ + K^+ + Ca^{2+} + Mg^{2+})$/TWSI.

correlated when the mass concentration of NH_3 was the highest (R^2 = 0.88) and the alkaline metal ion content was the lowest (R^2 = 0.93). With increasing mass concentration of NH_3, the regression slope increases and the intercept with the axis of $[NH_4^+]/[SO_4^{2-}]$ also becomes much closer to 2, suggesting more efficient homogeneous reaction between NH_3 and HNO_3 (Squizzato et al., 2013). As the mass fraction of alkaline metal ions decreases, a phenomenon similar to NH_3 influence is observed. We hypothesize that when NH_3 concentration is low, the alkaline metal ions such as Ca^{2+} and K^+ will compete with NH_3 for the formation of SO_4^{2-} and NO_3^- in the particle phase. As a result, a fraction of SO_4^{2-} will combine with alkaline metal ions, thereby decreasing the value of $[NH_4^+]/[SO_4^{2-}]$ and resulting in a smaller intercept value. On the other hand, a fraction of NO_3^- will combine with alkaline metal ions such as Ca^{2+}, leading to the existence of some data points in the ammonium-poor range with a relatively higher concentration of NO_3^-. Previous studies have also reported that nitrate may form on the reactive surfaces of particles, such as crustal dust, which act as reactive sinks for HNO_3 via heterogeneous chemistry (Dentener et al., 1996; Zhuang et al., 1999; Underwood et al., 2001; Yeatman et al., 2001; Lee et al., 2008). Under those conditions, the alkaline cations can decrease the aerosol acidity and drive HNO_3 into the aerosol phase, facilitating formation of particulate NO_3^- (Allen et al., 2015). This result indicates that the alkaline metal ions have an important influence in the formation of nitrate, especially when NH_3 concentration is low.

The relationships between mass fractions of sulfate ($m(SO_4^{2-})/m$(TWSI)) and nitrate ($m(NO_3^-)/m$(TWSI)) among total water-soluble ions (TWSI) in different ranges of alkaline metal ion content are shown in Fig. 6. Negative correlations were observed between $m(SO_4^{2-})/m$(TWSI) and $m(NO_3^-)/m$(TWSI) in all ranges of alkaline metal ion content, similar to Kong et al. (2014). These negative relationships may be due to the competition for NH_3 in the SO_4^{2-} and NO_3^- formation. From a qualitative standpoint, the reduction of sulfate can free up some NH_3 to react with HNO_3 and convert both to the particle phase, resulting in higher fractions of particulate nitrate. When the mass fraction of alkaline metal ion content increases, the mass fractions of NO_3^- and SO_4^{2-} decrease, with the former decreasing more than the latter, leading to a less negative slope (from −0.75 to −0.65) in the three ranges (Fig. 6). In addition, $m(SO_4^{2-})/m$(TWSI) and $m(NO_3^-)/m$(TWSI) become slightly less correlated when alkaline metal ion content increases (R^2 decreased from 0.87 to 0.67). This result suggests that under the conditions of dust storm or abundant fugitive dust from e.g., construction, alkaline metal ions can deteriorate the negative correlation trend between the mass fractions of SO_4^{2-} and NO_3^- due to the competition reactions from alkaline metals ions.

4. Conclusions

We investigated the roles of NH_3 and alkaline metal ions (Na^+, K^+, Ca^{2+}, and Mg^{2+}) in particulate sulfate and nitrate formation in Beijing through semi-continuous measurements of these species in winter. Both sulfate and nitrate mass concentrations showed exponential relationships with the partitioning ratio of ammonium $\varepsilon(NH_4^+)$. Sulfate mass concentration also showed strong dependence on RH, with more sulfate formation under high RH conditions, while such a RH dependence was not obvious for nitrate. The strong dependence of sulfate production on RH is also supported by a much larger increase (4 times) of SOR when comparing result at RH >50% to that at RH <50%, while NOR increase was only 2.4 times. The intercept of $[NH_4^+]/[SO_4^{2-}]$ in the $[NO_3^-]/[SO_4^{2-}]$ versus $[NH_4^+]/[SO_4^{2-}]$ plot was 0.9, indicating an NH_3-poor condition prevailed. By segregating the data points into different mass fraction ranges of alkaline metal ions, we showed that the role of NH_3 was replaced by alkaline ions in the neutralization reaction of H_2SO_4 and HNO_3 to form particulate SO_4^{2-} and NO_3^-. The relationships between mass fractions of SO_4^{2-} and NO_3^- in those ranges of different alkaline metal ion content also suggested that alkaline metal ions participate in the competing neutralization reaction of sulfate and nitrate.

Since sulfate and nitrate are still major inorganic species in fine PM in urban areas in China, mitigating these species requires implementation of effective control policies on their precursors (Y. Wang et al., 2013; Huang et al., 2014a; Chen et al., 2016). The increasing emissions of NH_3 might jeopardize the goal of PM reduction (Fu et al., 2017). However, our results suggest that alkaline metals can also facilitate sufficient neutralization reaction of H_2SO_4/HNO_3 even under NH_3-poor

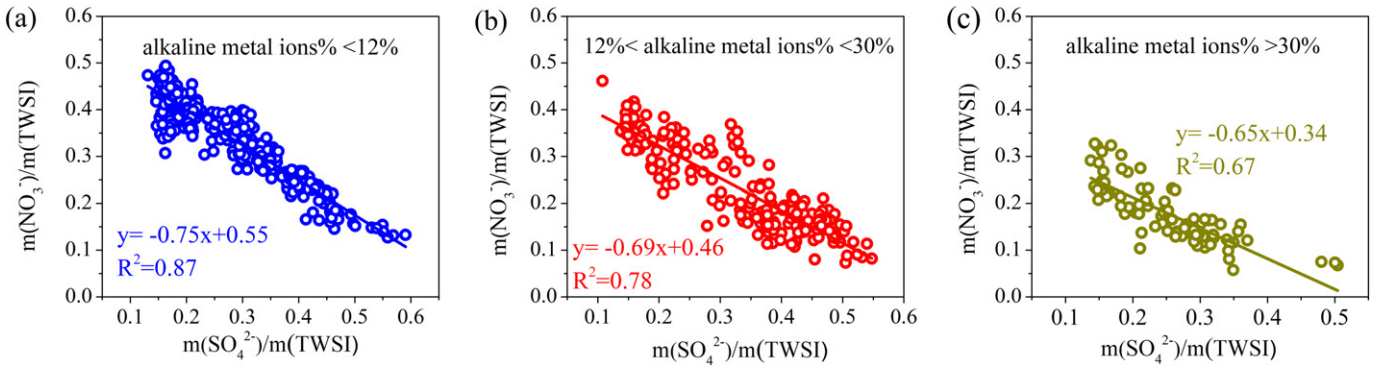

Fig. 6. Correlations between mass fractions of sulfate and nitrate in different alkaline metal ion content.

conditions. This finding implies that in some regions the chemistry to incorporate sulfur and nitrogen into the particle phase might be largely affected by desert/fugitive dust and sea salt, besides NH_3. This implication is particularly relevant in coastal areas of China and those areas with strong influence of dust particles in the North China Plain (NCP). The competition between sulfate and nitrate formation with regard to different alkaline metal ion content and aerosol acidity was also evident in our study. Given their vast difference in hygroscopicity and phase state (Martin, 2000; Li et al., 2017a), further investigation is also needed to understand exactly how their neutralization reaction is modulated by alkaline contents including ammonia and alkaline metals.

Supplementary data to this article can be found online at https://doi.org/10.1016/j.scitotenv.2020.137190.

Declaration of competing interest

The authors declare no competing financial interest.

Acknowledgments

This work was supported by the National Natural Science Foundation of China (NSFC) under Grant No. 41925015, 91644219, 91544107 and 41675120, the National Key Research and Development Program of China (No. 2017YFC0212701), the Chinese Academy of Sciences (no. ZDBS-LY-DQC001), and the Cross Innovative Team fund from the State Key Laboratory of Loess and Quaternary Geology (SKLLQG) (no. SKLLQGTD1801).

References

Allen, H.M., Draper, D.C., Ayres, B.R., Ault, A.P., Bondy, A.L., Takahama, S., Modini, R.L., Baumann, K., Edgerton, E., Knote, C., Laskin, A., Wang, B., Fry, J.L., 2015. Influence of crustal dust and sea spray supermicron particle concentrations and acidity on inorganic NO3− aerosol during the 2013 Southern Oxidant and Aerosol Study. Atmos. Chem. Phys. 15, 10669–10685.

Ansari, A.S., Pandis, S.N., 2000. The effect of metastable equilibrium states on the partitioning of nitrate between the gas and aerosol phases. Atmos. Environ. 34, 157–168.

Battaglia Jr., M.A., Weber, R.J., Nenes, A., Hennigan, C.J., 2019. Effects of water-soluble organic carbon on aerosol pH. Atmos. Chem. Phys. 19, 14607–14620.

Behera, S.N., Sharma, M., 2010. Investigating the potential role of ammonia in ion chemistry of fine particulate matter formation for an urban environment. Sci. Total Environ. 408, 3569–3575.

Behera, S.N., Betha, R., Balasubramanian, R., 2013. Insights into chemical coupling among acidic gases, ammonia and secondary inorganic aerosols. Aerosol Air Qual. Res. 13, 1282–1296.

Chen, D., Liu, Z.Q., Fast, J., Ban, J.M., 2016. Simulations of sulfate-nitrate-ammonium (SNA) aerosols during the extreme haze events over northern China in October 2014. Atmos. Chem. Phys. 16, 10707–10724.

Chow, J.C., Watson, J.G., 1998. Guideline on Speciated Particulate Monitoring. Report Prepared for US Environmental Protection Agency, Research Triangle Park, NC. by. Desert Research Institute, Reno, NV.

Dall'Osto, M., Harrison, R.M., Coe, H., Williams, P., 2009. Real-time secondary aerosol formation during a fog event in London. Atmos. Chem. Phys. 9, 2459–2469.

Dentener, F.J., Carmichael, G.R., Zhang, Y., Lelieveld, J., Crutzen, P.J., 1996. Role of mineral aerosol as a reactive surface in the global troposphere. J. Geophys. Res. Atmos. 101, 22869–22889.

Du, H.H., Kong, L.D., Cheng, T.T., Chen, J.M., Yang, X., Zhang, R.Y., Han, Z.W., Yan, Z., Ma, Y.L., 2010. Insights into ammonium particle-to-gas conversion: non-sulfate ammonium coupling with nitrate and chloride. Aerosol Air Qual. Res. 10, 589–595.

Du, H.H., Kong, L.D., Cheng, T.T., Chen, J.M., Du, J.F., Li, L., Xia, X., Leng, C., Huang, G., 2011. Insights into summertime haze pollution events over Shanghai based on online water-soluble ionic composition of aerosols. Atmos. Environ. 45, 5131–5137.

Fountoukis, C., Nenes, A., 2007. ISORROPIA II: a computationally efficient thermodynamic equilibrium model for K+–Ca2+–Mg2+–NH4+–Na+–SO42−–NO3−–Cl−–H2O aerosols. Atmos. Chem. Phys. 7, 4639–4659.

Fu, X., Wang, S.X., Xing, J., Zhang, X.Y., Wang, T., Hao, J.M., 2017. Increasing ammonia concentrations reduce the effectiveness of particle pollution control achieved via SO2 and NOX emissions reduction in east China. Environ. Sci. Tech. Lett. 4, 221–227.

Ge, X.L., Wexler, A.S., Clegg, S.L., 2011. Atmospheric amines - part I, a review. Atmos. Environ. 45, 524–546.

Ge, X.L., He, Y.A., Sun, Y.L., Xu, J.Z., Wang, J.F., Shen, Y.F., Chen, M.D., 2017. Characteristics and formation mechanisms of fine particulate nitrate in typical urban areas in China. Atmosphere 8, 62.

Griffith, S.M., Huang, X., Louie, P.K., Yu, J.Z., 2015. Characterizing the thermodynamic and chemical composition factors controlling PM 2.5 nitrate: insights gained from two years of online measurements in Hong Kong. Atmos. Environ. 122, 864–875.

Guo, H., Xu, L., Bougiatioti, A., Cerully, K.M., Capps, S.L., Hite Jr., J.R., Carlton, A.G., Lee, S.-H., Bergin, M.H., Ng, N.L., Nenes, A., Weber, R.J., 2015. Fine-particle water and pH in the southeastern United States. Atmos. Chem. Phys. 15, 5211–5228.

Guo, H., Sullivan, A.P., Campuzano-Jost, P., Schroder, J.C., Lopez-Hilfiker, F.D., Dibb, J.E., Jimenez, J.L., Thornton, J.A., Brown, S.S., Nenes, A., Weber, R.J., 2016. Fine particle pH and the partitioning of nitric acid during winter in the northeastern United States. J. Geophys. Res. 121, 10355–10376.

Guo, H., Nenes, A., Weber, R.J., 2018. The underappreciated role of nonvolatile cations in aerosol ammonium-sulfate molar ratios. Atmos. Chem. Phys. 18, 17307–17323.

He, K., Zhao, Q., Ma, Y., Duan, F., Yang, F., Shi, Z., Chen, G., 2012. Spatial and seasonal variability of PM2.5 acidity at two Chinese megacities: insights into the formation of secondary inorganic aerosols. Atmos. Chem. Phys. 12, 25557–25603.

Hennigan, C.J., Izumi, J., Sullivan, A.P., Weber, R.J., Nenes, A., 2015. A critical evaluation of proxy methods used to estimate the acidity of atmospheric particles. Atmos. Chem. Phys. 15, 2775–2790.

Hertel, O., Skjoth, C.A., Reis, S., Bleeker, A., Harrison, R.M., Cape, J.N., Fowler, D., Skiba, U., Simpson, D., Jickells, Kulmala, T.M., Gyldenkærne, S., Sørensen, L.L., Erisman, J.W., Sutton, M.A., 2012. Governing processes for reactive nitrogen compounds in the European atmosphere. Biogeosciences 9, 4921–4954.

Hu, M., Wu, Z.J., Slanina, J., Lin, P., Liu, S., Zeng, L.M., 2008. Acidic gases, ammonia and water-soluble ions in PM2.5 at a coastal site in the Pearl River Delta, China. Atmos. Environ. 42, 6310–6320.

Huang, X., Qiu, R., Chan, C.K., Kant, P.R., 2011. Evidence of high PM2.5 strong acidity in ammonia-rich atmosphere of Guangzhou, China: transition in pathways of ambient ammonia to form aerosol ammonium at [NH4+]/[SO42-] = 1.5. Atmos. Res. 99, 488–495.

Huang, Y.L., Chen, H., Wang, L., Yang, X., Chen, J.M., 2012. Single particle analysis of amines in ambient aerosol in Shanghai. Environ. Chem. 9, 202–210.

Huang, R.J., Zhang, Y.L., Bozzetti, C., Ho, K.F., Cao, J.J., Han, Y.M., Daellenbach, K.R., Slowik, J.G., Platt, S.M., Canonaco, F., Zotter, P., Wolf, R., Pieber, S.M., Bruns, E.A., Crippa, M., Ciarelli, G., Piazzalunga, A., Schwikowski, M., Abbaszade, G., Schnelle-Kreis, J., Zimmermann, R., An, Z., Szidat, S., Baltensperger, U., Haddad, I.E., Prevot, A.S.H., 2014a. High secondary aerosol contribution to particulate pollution during haze events in China. Nature 514, 218–222.

Huang, R.J., Li, W.B., Wang, Y.R., Wang, Q.Y., Jia, W.T., Ho, K.F., Cao, J.J., Wang, G.H., Chen, X., El Haddad, I., Zhuang, Z.X., Wang, X.R., Prévôt, A.S.H., O'Dowd, C.D., Hoffmann, T., 2014b. Determination of aliphatic amines in atmospheric aerosol particles: a comparison of gas chromatography-mass spectrometry and ion chromatography approaches. Atmos. Meas. Tech. 7, 2027–2035.

Ianniello, A., Spataro, F., Esposito, G., Allegrini, I., Rantica, E., Ancora, M.P., Hu, M., Zhu, T., 2010. Occurrence of gas phase ammonia in the area of Beijing (China). Atmos. Chem. Phys. 10, 9487–9503.

Khlystov, A., Wyers, G.P., Slanina, J., 1995. The steam-jet aerosol collector. Atmos. Environ. 29, 2229–2234.

Khoder, M.I., 2002. Atmospheric conversion of sulfur dioxide to particulate sulfate and nitrogen dioxide to particulate nitrate and gaseous nitric acid in an urban area. Chemosphere 49, 675–684.

Kong, L.D., Yang, Y.W., Zhang, S.Q., Zhao, X., Du, H.H., Fu, H.B., Zhang, S.C., Cheng, T.T., Yang, X., Chen, J.M., Wu, D., Shen, J.D., Hong, S.M., Jiao, L., 2014. Observations of linear dependence between sulfate and nitrate in atmospheric particles. J. Geophys. Res. Atmos. 119, 341–361.

Lee, T., Yu, X.Y., Ayres, B., Kreidenweis, S.M., Malm, W.C., Jr, J.L.C., 2008. Observations of fine and coarse particle nitrate at several rural locations in the United States. Atmos. Environ. 42, 2720–2732.

Li, Y.J., Liu, P.F., Bergoend, C., Bateman, A.P., Martin, S.T., 2017a. Rebounding hygroscopic inorganic aerosol particles: liquids, gels, and hydrates. Aerosol Sci. Technol. 51, 388–396.

Li, Y.J., Sun, Y., Zhang, Q., Li, X., Li, M., Zhou, Z., Chan, C.K., 2017b. Real-time chemical characterization of atmospheric particulate matter in China: a review. Atmos. Environ. 158, 270–304.

Maasikmets, M., Teinemaa, E., Kaasik, A., Kimmel, V., 2015. Measurement and analysis of ammonia, hydrogen sulphide and odour emissions from the cattle farming in Estonia. Biosyst. Eng. 139, 48–59.

Martin, S.T., 2000. Phase transitions of aqueous atmospheric particles. Chem. Rev. 100, 3403–3453.

Mentel, T.F., Sohn, M., Wahner, A., 1999. Nitrate effect in the heterogeneous hydrolysis of dinitrogen pentoxide on aqueous aerosols. Phys. Chem. Chem. Phys. 1, 5451–5457.

Nenes, A., Pandis, S.N., Weber, R.J., Russell, A., 2019. Aerosol pH and liquid water content determine when particulate matter is sensitive to ammonia and nitrate availability. Atmos. Chem. Phys. Discuss. https://doi.org/10.5194/acp-2019-840 (review).

Nie, W., Ding, A.J., Xie, Y.N., Xu, Z., Mao, H., Kerminen, V.M., Zheng, L.F., Qi, X.M., Huang, X., Yang, X.Q., 2015. Influence of biomass burning plumes on HONO chemistry in eastern China. Atmos. Chem. Phys. 15, 1147–1159.

Pathak, R.K., Wu, W.S., Wang, T., 2009. Summertime PM2.5 ionic species in four major cities of China: nitrate formation in an ammonia-deficient atmosphere. Atmos. Chem. Phys. 9, 1711–1722.

Pye, H.O.T., Nenes, A., Alexander, B., Ault, A.P., Barth, M.C., Clegg, S.L., Collett Jr., J.L., Fahey, K.M., Hennigan, C.J., Herrmann, H., Kanakidou, M., Kelly, J.T., Ku, I.-T., McNeill, V.F., Riemer, N., Schaefer, T., Shi, G., Tilgner, A., Walker, J.T., Wang, T., Weber, R., Xing, J., Zaveri, R.A., Zuend, A., 2019. The acidity of atmospheric particles and clouds. Atmos. Chem. Phys. Discuss. https://doi.org/10.5194/acp-2019-889 (review).

Rumsey, I.C., Cowen, K.A., Walker, J.T., Kelly, T.J., Hanft, E.A., Mishoe, K., Rogers, C., Proost, R., Beachley, G.M., Lear, G., Frelink, T., Otjes, R.P., 2014. An assessment of the performance of the Monitor for AeRosols and GAses in ambient air (MARGA): a semi-continuous method for soluble compounds. Atmos. Chem. Phys. 14, 5639–5658.

Ryu, S.Y., Kwon, B.G., Kim, Y.J., Kim, H.H., Chun, K.J., 2007. Characteristics of biomass burning aerosol and its impact on regional air quality in the summer of 2003 at Gwangju, Korea. Atmos. Res. 84 (4), 362–373.
Sander, S.P., Seinfeld, J.H., 1976. Chemical kinetics of homogeneous atmospheric oxidation of sulfur dioxide. Environ. Sci. Technol. 10, 1114–1123.
Seinfeld, J.H., Pandis, S.N., 2016. Atmospheric Chemistry and Physics: From Air Pollution to Climate Change. 3rd Ed. John Wiley & Sons, Inc.
Sharma, M., Kishore, S., Tripathi, S.N., Behera, S.N., 2007. Role of atmospheric ammonia in the formation of inorganic secondary particulate matter: a study at Kanpur, India. J. Atmos. Chem. 58, 1–17.
Silvern, R.F., Jacob, D.J., Kim, P.S., Marais, E.A., Turner, J.R., Campuzano-Jost, P., Jimenez, J.L., 2017. Inconsistency of ammonium-sulfate aerosol ratios with thermodynamic models in the eastern US: a possible role of organic aerosol. Atmos. Chem. Phys. 17, 5107–5118.
Song, S., Gao, M., Xu, W., Shao, J., Shi, G., Wang, S., Wang, Y., Sun, Y., McElroy, M.B., 2018. Fine-particle pH for Beijing winter haze as inferred from different thermodynamic equilibrium models. Atmos. Chem. Phys. 18, 7423–7438.
Squizzato, S., Masiol, M., Brunelli, A., Pistollato, S., Tarabotti, E., Rampazzo, G., Pavoni, B., 2013. Factors determining the formation of secondary inorganic aerosol: a case study in the Po Valley (Italy). Atmos. Chem. Phys. 13, 1927–1939.
Sun, Y.L., Wang, Z.F., Fu, P.Q., Jiang, Q., Yang, T., Li, J., Ge, X.L., 2013. The impact of relative humidity on aerosol composition and evolution processes during wintertime in Beijing, China. Atmos. Environ. 77, 927–934.
Sun, Y.L., Jiang, Q., Wang, Z.F., Fu, P.Q., Li, J., Yang, T., Yin, Y., 2014. Investigation of the sources and evolution processes of severe haze pollution in Beijing in January 2013. J. Geophys. Res. Atmos. 119, 4380–4398.
Takegawa, N., Miyakawa, T., Kuwata, M., Kondo, Y., Zhao, Y., Han, S., Kita, K., Miyazaki, Y., Deng, Z., Xiao, R., Hu, M., van Pinxteren, D., Herrmann, H., Hofzumahaus, A., Holland, F., Wahner, A., Blake, D.R., Sugimoto, N., Zhu, T., 2009. Variability of submicron aerosol observed at a rural site in Beijing in the summer of 2006. J. Geophys. Res. Atmos. 114, 1291–1298.
Tan, H.B., Cai, M.F., Fan, Q., Liu, L., Li, F., Chan, P.W., Deng, X.J., Wu, D., 2017. An analysis of aerosol liquid water content and related impact factors in Pearl River Delta. Sci. Total Environ. 579, 1822–1830.
Tang, M.J., Thieser, J., Schuster, G., Crowley, J.N., 2012. Kinetics and mechanism of the heterogeneous reaction of N2O5 with mineral dust particles. Phys. Chem. Chem. Phys. 14, 8551–8561.
Tao, Y., Ye, X., Ma, Z., Xie, Y., Wang, R., Chen, J., Jiang, S., 2016. Insights into different nitrate formation mechanisms from seasonal variations of secondary inorganic aerosols in Shanghai. Atmos. Environ. 145, 1–9.
Ten Brink, H., Otjes, R., Jongejan, P., Slanina, S., 2007. An instrument for semi-continuous monitoring of the size-distribution of nitrate, ammonium, sulphate and chloride in aerosol. Atmos. Environ. 41, 2768–2779.
Tian, M., Wang, H.B., Chen, Y., Yang, F.M., Zhang, X.H., Zou, Q., Zhang, R.Q., Ma, Y.L., He, K.B., 2016. Characteristics of aerosol pollution during heavy haze events in Suzhou, China. Atmos. Chem. Phys. 16, 7357–7371.
Trebs, I., Meixner, F.X., Slanina, J., Otjes, R., Jongejan, P., Andreae, M.O., 2004. Real-time measurements of ammonia, acidic trace gases and water-soluble inorganic aerosol species at a rural site in the Amazon Basin. Atmos. Chem. Phys. 4, 967–987.
Trebs, I., Metzger, S., Meixner, F.X., Helas, G., Hoffer, A., Rudich, Y., Falkovich, A.H., Moura, M.A.L., Jr, R.S.D.S., Artaxo, P., 2005. The NH4+-NO3−-Cl−-SO42−-H2O aerosol system and its gas phase precursors at a pasture site in the Amazon Basin: how relevant are mineral cations and soluble organic acids? J. Geophys. Res. Atmos. 110, 1275–1287.
Underwood, G.M., Song, C.H., Phadnis, M., Carmichael, G.R., Grassian, V.H., 2001. Heterogeneous reactions of NO2 and HNO3 on oxides and mineral dust: a combined laboratory and modeling study. J. Geophys. Res. Atmos. 106, 18055–18066.
Vasilakos, P., Russell, A., Weber, R., Nenes, A., 2018. Understanding nitrate formation in a world with less sulfate. Atmos. Chem. Phys. 18, 12765–12775.
Wakamatsu, S., Utsunomiya, A., Jin, S.H., Mori, A., Uno, I., Uehara, K., 1996. Seasonal variation in atmospheric aerosols concentration covering northern Kyushu, Japan and Seoul, Korea. Atmos. Environ. 30, 2343–2354.
Wang, L., Du, H.H., Chen, J.M., Zhang, M., Huang, X.Y., Tan, H.B., Kong, L.D., Geng, F.H., 2013a. Consecutive transport of anthropogenic air masses and dust storm plume: two case events at Shanghai, China. Atmos. Res. 127, 22–33.
Wang, Y., Zhang, Q.Q., He, K., Zhang, Q., Chai, L., 2013b. Sulfate-nitrate-ammonium aerosols over China: response to 2000-2015 emission changes of sulfur dioxide, nitrogen oxides, and ammonia. Atmos. Chem. Phys. 13, 2635–2652.
Wang, G.H., Zhang, R.Y., Gomez, M.E., Yang, L.X., Zamora, M.L., Hu, M., Lin, Y., Peng, J.F., Guo, S., Meng, J.J., Li, J.J., Cheng, C.L., Hu, T.F., Ren, Y.Q., Wang, Y.S., Gao, J., Cao, J.J., An, Z.S., Zhou, W.J., Li, G.H., Wang, J.Y., Tian, P.F., Marrero-Ortiz, W., Secrest, J., Du, Z.F., Zheng, J., Shang, D.J., Zeng, L.M., Shao, M., Wang, W.G., Huang, Y., Wang, Y., Zhu, Y.J., Li, Y.X., Hu, J.X., Pan, B., Cai, L., Cheng, Y.T., Ji, Y.M., Zhang, F., Rosenfeld, D., Liss, P.S., Duce, R.A., Kolb, C.E., Molina, M.J., 2016. Persistent sulfate formation from London Fog to Chinese haze. Proc. Natl. Acad. Sci. U. S. A. 113, 13630–13635.
Willison, M.J., Clarke, A.G., Zeki, E.M., 1985. Seasonal variation in atmospheric aerosol concentration and composition at urban and rural sites in northern England. Atmos. Environ. 19, 1081–1089.
Xiao, R., Takegawa, N., Kondo, Y., Miyazaki, Y., Miyakawa, T., Hu, M., Shao, M., Zeng, L.M., Hofzumahaus, A., Holland, F., Lu, K., Sugimoto, N., Zhao, Y., Zhang, Y.H., 2009. Formation of submicron sulfate and organic aerosols in the outflow from the urban region of the Pearl River Delta in China. Atmos. Environ. 43, 3754–3763.
Yang, Y.R., Liu, X.G., Qu, Y., An, J.L., Jiang, R., Zhang, Y.H., Sun, Y.L., Wu, Z.J., Zhang, F., Xu, W.Q., Ma, Q.X., 2015. Characteristics and formation mechanism of continuous hazes in China: a case study during the autumn of 2014 in the North China Plain. Atmos. Chem. Phys. 15, 8165–8178.
Yao, X.H., Fang, M., Chan, C.K., 2001. Experimental study of the sampling artifact of chloride depletion from collected sea salt aerosols. Environ. Sci. Technol. 35, 600–605.
Ye, X.N., Ma, Z., Zhang, J.C., Du, H.H., Chen, J.M., Chen, H., Yang, X., Gao, W., Geng, F.H., 2011. Important role of ammonia on haze formation in Shanghai. Environ. Res. Lett. 6, 024019.
Yeatman, S.G., Spokes, L.J., Jickells, T.D., 2001. Comparisons of coarse-mode aerosol nitrate and ammonium at two polluted coastal sites. Atmos. Environ. 35, 1321–1335.
Zhang, G.H., Bi, X.H., Chan, L.Y., Li, L., Wang, X.M., Feng, J.L., Sheng, G.Y., Fu, J.M., Li, M., Zhou, Z., 2012. Enhanced trimethylamine-containing particles during fog events detected by single particle aerosol mass spectrometry in urban Guangzhou, China. Atmos. Environ. 55, 121–126.
Zhang, Q., Shen, Z., Cao, J., Ho, K., Zhang, R., Bie, Z., Chang, H., Liu, S., 2014. Chemical profiles of urban fugitive dust over Xi'an in the south margin of the Loess Plateau, China. Atmos. Pollut. Res. 5 (3), 421–430.
Zheng, B., Zhang, Q., Zhang, Y., He, K.B., Wang, K., Zheng, G.J., Duan, F.K., Ma, Y.L., Kimoto, T., 2015a. Heterogeneous chemistry: a mechanism missing in current models to explain secondary inorganic aerosol formation during the January 2013 haze episode in North China. Atmos. Chem. Phys. 15, 2031–2049.
Zheng, G.J., Duan, F.K., Su, H., Ma, Y.L., Cheng, Y., Zheng, B., Zhang, Q., Huang, T., Kimoto, T., Chang, D., Poschl, U., Cheng, Y.F., He, K.B., 2015b. Exploring the severe winter haze in Beijing: the impact of synoptic weather, regional transport and heterogeneous reactions. Atmos. Chem. Phys. 15, 2969–2983.
Zheng, J., Ma, Y., Chen, M.D., Zhang, Q., Wang, L., Khalizov, A.F., Yao, L., Wang, Z., Wang, X., Chen, L.X., 2015c. Measurement of atmospheric amines and ammonia using the high resolution time-of-flight chemical ionization mass spectrometry. Atmos. Environ. 102, 249–259.
Zhuang, H., Chan, C.K., Fang, M., Wexler, A.S., 1999. Formation of nitrate and non-sea-salt sulfate on coarse particles. Atmos. Environ. 33, 4223–4233.